Networking Study of Waveband/Wavelength Switching for Multi-Granular and Multi-Band Optical Networks

Networking Study of Waveband/Wavelength Switching for Multi-Granular and Multi-Band Optical Networks

Muhammad Umar Masood
Politecnico di Torino, IT
muhammad.masood@polito.it

Ihtesham Khan
Politecnico di Torino, IT
ihtesham.khan@polito.it

Lorenzo Tunesi
Politecnico di Torino, IT
lorenzo.tunesi@polito.com

Andrea Marchisio
Politecnico di Torino, IT
andrea.marchisio@polito.it

Enrico Ghillino
Synopsys, USA
enrico.ghillino@synopsys.com

Paolo Bardella
Politecnico di Torino, IT
paolo.bardella@polito.it

Andrea Carena
Politecnico di Torino, IT
andrea.carena@polito.it

Vittorio Curri
Politecnico di Torino, IT
curri@polito.it

***Abstract*—In the imminent era of bandwidth-abundant optical networks, the concept of hierarchical optical network architectures emerges, decoupling the massive spatial division multiplexing (SDM) layer and the wavelength division multiplexing layer. In this paper, we perform a networking-level analysis of a generalized multiband optical cross-connect (OXC) that realizes switching in two steps: grouping wavelengths and switching them as waveband paths. The performed analysis is simulated for multiband and SDM systems, demonstrating that while conventional single-layer wavelength routing remains effective under certain conditions, waveband routing offers a more scalable and cost-effective solution under specific high-load conditions in bandwidth-abundant optical networks. This positions waveband routing as a promising alternative for future high-capacity networks.**

***Index Terms*—Hierarchical optical network; Waveband paths; Spatial division multiplexing; Multi-band transmission.**

I. Introduction

Optical networks form the backbone of modern information and communication technology ecosystems, primarily due to their unparalleled bandwidth capacity and minimal latency. The relentless surge in internet traffic, propelled by the advent of technologies such as 5G/6G communications, high-bandwidth video streaming services, and cloud computing, has pushed the boundaries of existing optical transmission systems [1]. To meet the demand for growing traffic, technologies such as dense wavelength division multiplexing (DWDM), digital coherent transmission, and the flexible ITU-T grid [2] enabled maximum capacity for the use of single-mode fibers (SMFs) and are reaching the theoretical limit [3], [4]. In response, the optical communication society has recently focused on exploiting additional low-loss spectrum windows, particularly C+L+S bands [5]. Furthermore, massive spatial parallelism by multicore fiber/parallel-SMF links [6] is also considered for future bandwidth-abundant optical networks.

The concept of multicore fiber/parallel-SMF can be implemented under the umbrella of a spatial division multiplexing (SDM) network, which requires not only multi-core/mode fibers [7] but also switching devices [8], amplifiers [9], and node architectures [10] to be developed to support this massive spatial parallelism. However, multi-band transmission (MBT) can be implemented at the expense of additional transmission loss and the usage of switching and amplifier devices that operate on a wide spectrum range [11]. In this context, the development of large-scale reconfigurable optical add/drop multiplexers (ROADMs) or optical cross-connects (OXCs) is significant to enable SDM/MBT-based networks [12] fully.

Today, most ROADMs/OXCs operate at wavelength-path granularity level and are developed with wavelength-selective switches (WSSs), having a maximum port count of 35 [13]. To enable them for the upcoming massive spatial parallelism networks, which will demand a high port count, one has to cascade multiple WSSs to fulfill the port count requirement. The number of these cascaded WSSs in a node is almost the square of the ROADMs/OXCs degree [12]. In addition, cascaded WSS accumulates more transmission loss at each stage; therefore, more amplifiers are necessary to compensate for this accumulated transmission loss, adding additional noise to the system. Moreover, network management in software-defined networks (SDN) can be much more difficult as the number of dynamic network services, such as dynamic optical path allocation, switched optical path/circuits, optical flows, and even optical burst/packet service, increases. Therefore, conventional single-layer wavelength (WL) switching will significantly increase cost and complexity as the optical transmission system progressively moves toward MBT and higher SDM transmission systems in the upcoming era of 6G communication [14]. To address these issues, the introduction of another optical layer, the waveband (WB) path, which is a collection of several wavelength paths, has been intensively investigated in recent years [15]–[18].

The WB layer groups various wavelength paths, where all grouped wavelengths of a WB are simultaneously routed as a single entity. Adopting this WB layer instead of conventional

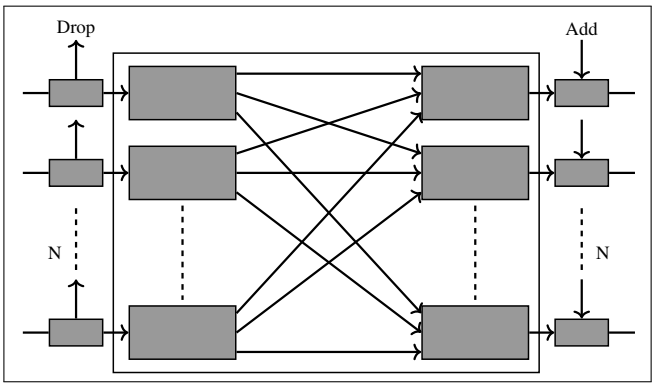

Fig. 1: Wavelength enabled node architecture

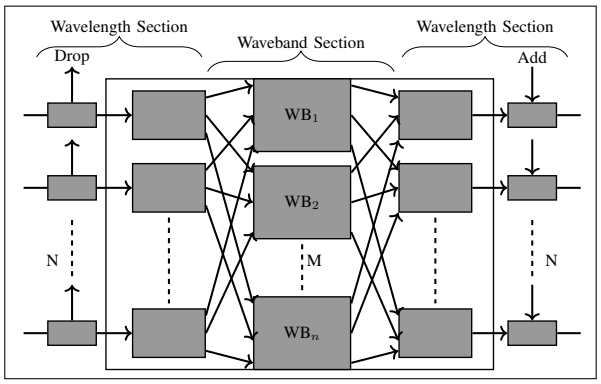

Fig. 2: Waveband enabled node architecture

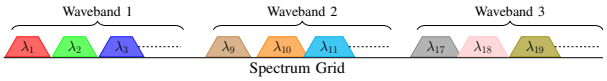

Fig. 3: Wavelengths arrangement to form waveband

WL switching has two main advantages. In single-layer architecture, the optical path requires node-by-node optical control. In multilayer architecture, only WB terminating nodes require signaling for wavelength-path establishment/release using one or several WBs. By adopting a multi-layer architecture, the switches involved in signaling and control are significantly reduced, subsequently reducing the path control delay, and signaling cost can be decreased. Another main benefit of the multilayer architecture is the reduction of hardware scale in developing OXCs. In the upcoming era of massive SDM, the OXC must accommodate numerous multicore fiber/parallel-SMF links. The current wavelength-granular-based OXCs architecture should cascade multiple costly WSS to make it compatible with the upcoming massive SDM era, because the commercial WSS port count is limited to 35+ [13]. A potential alternative to this costly solution is WB switching, which is more cost-effective and simple, as demonstrated in [19].

This paper performs a networking-level analysis of generic OXCs. The routing scheme of the considered switching system is realized in two steps: grouping WLs to form WBs and switching these WB paths. Small continuous WLs are grouped for each input port and form a WB. The grouped WLs in the WB path are switched together, keeping the continuity and contiguity constrained. The simulation is performed in two steps. Initially, the analysis is performed only for the multiband system, including the spectrum windows of the C+L+S bands. Subsequently, the study is extended to a multicore fiber/parallel-SMF transmission system to cope with the upcoming bandwidth-abundant system. The node architecture considered in this analysis is proposed in [20], in which small-port-count WSSs for two frequency bands (C+L) are used as dynamic optical filters to form WBs. In this work, instead of using separate WSSs for the (C+L) bands, a single modular multiband WSS is considered, which can operate in low-loss regions, i.e., C+L+S bands [11]. The analysis performed in this work shows that conventional WL routing is no longer feasible for upcoming bandwidth-abundant optical networks; the potential alternative to traditional WL routing is the cost-effective and straightforward WB routing.

II. Waveband-Enabled Node and Resource Assignment in Waveband Networks

The conventional WL-based switching system utilizes the traditional granular wavelength routing method, as shown in Fig. 1. The main component of this architecture is WSS, which performs the switch and add/drop functionality. Similarly, Fig 2, shows the coarse granular routing scheme, i.e., WB routing. In this WB granularity, the routing operation involves three main steps: Initially, the optical paths of the incoming fibers are grouped into n WBs. The construction of WB follows the continuity and contiguity constraints of WL shown in Fig. 3. Then, n WBs are routed independently to the connected outgoing fiber port. Lastly, the WBs arriving at any fiber port are coupled to deliver WBs to more outgoing fibers. This investigation only performs the networking level analysis of OXCs architecture; the device-level functionality and architecture are beyond the scope of this article, which has previously been well analyzed in [21].

To efficiently allocate resources in waveband networks and facilitate the deployment of new connection requests in the form of lightpaths (LPs), we propose a structured algorithm, detailed as follows:

Initially, the algorithm checks for any existing lightpaths between the source (s) and destination (d) nodes that have sufficient spare capacity to accommodate the requested traffic (t). This step is illustrated in line 1 of Alg. 1.

If no suitable existing lightpath is found, the algorithm proceeds to establish a new lightpath. It sequentially evaluates each of the k possible routes between the node pair (as shown in line 4). For each selected route (r), the algorithm identifies available free channels, grouping them into sets of M channels (line 10).

Algorithm 1 Resource assignment

Require: $RS_{i,j}$: Route space for all network node pairs (i, j), M: number of channels to compose the waveband, $c(s, d, t)$: new connection request (c) containing source (s) and destination (d) nodes, and traffic (t)

1: try allocation of c in already deployed LPs
2: **if** c is not allocated **then**
3: $R \leftarrow RS_{s,d}$
4: **while** $R \neq \emptyset$ **and** c not allocated **do**
5: $r \leftarrow$ first route from R
6: $R \leftarrow R \setminus r$
7: $c(s, d, t, r) \leftarrow c(s, d, t) \cup r$
8: $T \leftarrow 0$
9: $n \leftarrow \emptyset$ {Set of channels used to allocate request c}
10: $H \leftarrow$ list of free channels in route r divided in sets of M channels
11: **while** $H \neq \emptyset$ **and** $T < t$ **do**
12: $h \leftarrow$ first set of M channels from H
13: $H \leftarrow H \setminus h$
14: $n \leftarrow n \cup h$
15: $i \leftarrow$ computation of bit rate of route r using channels in h (GSNR based)
16: $T \leftarrow T + i$
17: **end while**
18: **if** $T \geq t$ **then**
19: $c(s, d, t, r, n) \leftarrow c(s, d, t, r) \cup n$
20: allocate c using channels in n through route r
21: **end if**
22: **end while**
23: **end if**

For each set of channels, the algorithm calculates the total bit rate, considering the modulation format that the Generalized Signal-to-Noise Ratio (GSNR) of these channels can support (line 15). The modulation format is chosen based on the required RGSNR for the transceiver [22].

Subsequently, the algorithm checks whether the total capacity of the selected channels (T) meets or exceeds the requested traffic volume. If this condition is satisfied, the connection is established using the identified channels within the chosen route (line 18).

This resource allocation algorithm adheres to the wavelength continuity and contiguity constraints, which are integral to conventional WL routing, where M is set to 1. The same principles are applied to WB routing, whether in multiband or multicore fiber/parallel single-mode fiber (SMF) contexts. This method ensures efficient resource utilization, optimizing network capacity and supporting the robust deployment of new services.

III. Networking Analysis

The network's overall performance should be studied to analyze the effect of the single-layer conventional WL and multilayer WB architecture on different optical transport setups. For this purpose, the statistical network assessment process (SNAP) [23] is exploited, which operates on the physical layer of the tested network and is based on the degradation in the Quality-of-Transmission (QoT) caused by each networking element. The QoT metric considered in this case is the generalized signal-to-noise ratio (GSNR) which accumulates both P_{ASE} and P_{NLI}, using

$$\mathrm{GSNR_i} = \frac{P_{\mathrm{S,i}}}{P_{\mathrm{ASE}(f_i)} + P_{\mathrm{NLI,i}}(f_i)}\,, \tag{1}$$

for the ith channel with center frequency f_i, where $P_{\mathrm{S,i}}$ is the transmitted power of the signal, $P_{\mathrm{ASE}(f_i)}$ is the amplified spontaneous emission, and $P_{\mathrm{NLI,i}}(f_i)$ is the non-linear interference of the fiber

The analysis is performed in two stages; initially, it is simulated for the multi-band optical system, and after that, the investigation is further extended to multi-core fiber/parallel-SMF. The multiband transmission system is constructed from a series of bands, with components, especially optical amplifiers, optimized for each band [24]. Each fiber in the amplified lines has the same length of 75 km, and the fiber

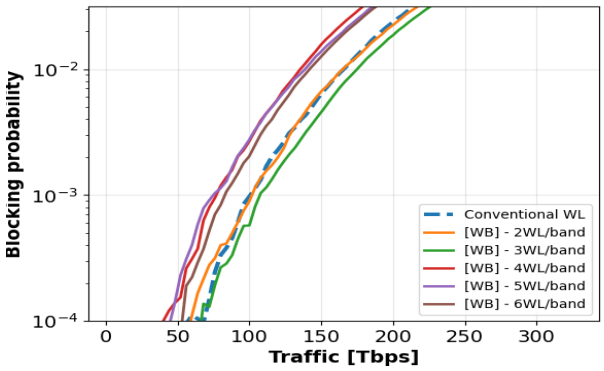

Fig. 4: Blocking probability vs. traffic for wavelength and waveband enabled C+L network.

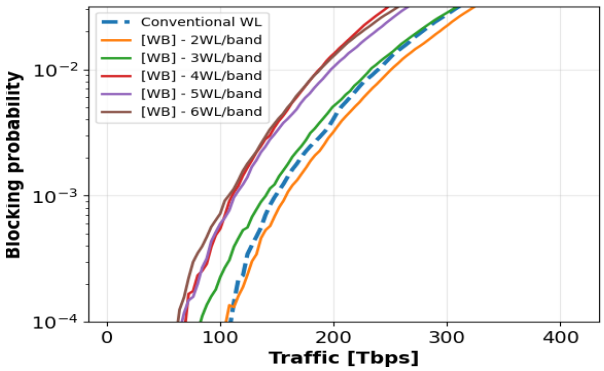

Fig. 5: Blocking probability vs. traffic for wavelength and waveband enabled C+L+S network.

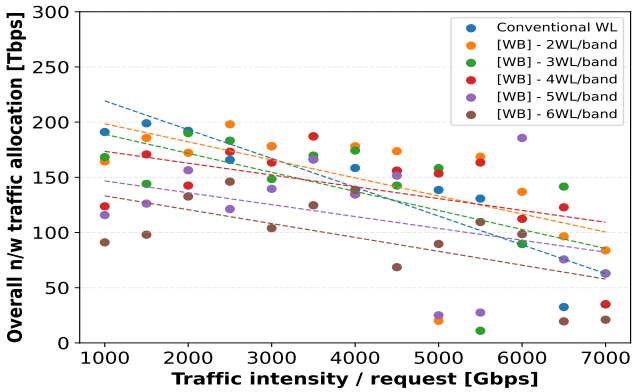

Fig. 6: Impact of waveband size (M) on overall C+L Network Traffic.

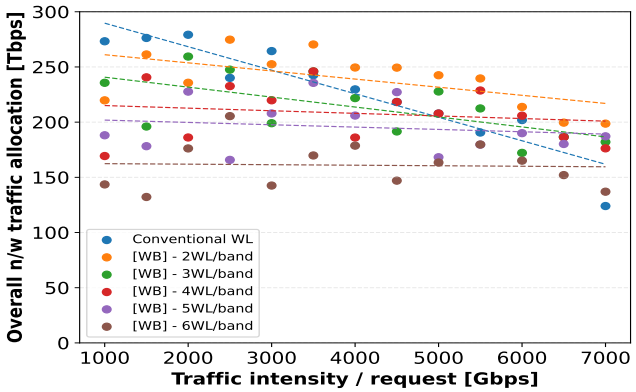

Fig. 7: Impact of waveband size (M) on overall C+L+S Network Traffic.

types used are standard single-mode fiber (ITU-T G.652D). The amplifiers considered for this analysis are commercially available erbium-doped fiber amplifiers (EDFAs) for C- and L-band and thulium-doped fiber amplifiers for the S-band [25]. The transceiver of 1200 G transmission with a Free Spectral Range (FSR) of 150 GHz, symbol rate of 130 GBaud is considered [26].

The input power for each band is optimized, following a span-by-span strategy using the local optimization global optimization (LOGO) algorithm based on maximizing QoT [27]. The simulation considered rationally loaded C, L, and S bands at FSR=150 GHz, which results in 105 channels (C band-25 (≈4 THz), L band-40 (6 THz), and S band-40 (6 THz) channels). Here, it is important to note that in C+L and S+C+L band scenarios, the average GSNR of the C-band and L-band is lower than the reference C-band transmission case, mainly due to the iterative impact of Stimulated Raman Scattering (SRS) and NLI [28]. Similarly, for the SDM system, the performed analysis considers parallel SMF fibers. The number of fibers is fixed to five to relax the computation complexity.

A single channel is routed at a given time for the conventional single-layer WL switching system. On the other hand, in the WB switching architecture, a continuous WL is grouped up first; the minimum 2WL/WB and maximum 6WL/WB are considered. The grouped WLs are routed as a single WB at a given time. This work considers the German network topology, having 17 optical nodes and 26 edges. The optical nodes represent the ROADMs/OXCs, where traffic requests are added/dropped, while the edges represent the optical line systems, including fiber pairs and in-line amplifiers. The network average node degree is 3.1, with an average inter-node distance of 207 km and a maximum link length of 300 km; furthermore, a uniform traffic distribution among all nodes in the network is considered for the performed simulation.

IV. Results

In order to evaluate the influence of the WB architecture on networking performance in comparison to the traditional WL architecture, an extensive series of simulations are conducted across various network scenarios.

Fig. 4 illustrates the distribution of network traffic across a spectrum of blocking probabilities (BP) for conventional WL and WB architectures ($M = 2, 3, 4, 5, 6$), with each scenario accommodating a uniform traffic load of 4000 Gbps per request, within the C+L spectrum. Whereas Fig. 5 shows the overall network allocation against the BP for the C+L+S scenario. In Fig. 4, for $BP = 10^{-2}$, the traffic allocation for the WL case is 166 Tbps. Compared to the WB case ($M = 2, 3, 4, 5, 6$), the overall traffic allocation is 164 Tbps (1.2% lower), 177 Tbps (6.63% higher), 136 Tbps (22.9% lower), 139 Tbps (15.66% lower), and 141 Tbps (14.4% lower), respectively. In Fig. 5, for $BP = 10^{-2}$, the traffic allocation for the WL case is 241.5 Tbps. Compared to the WB case ($M = 2, 3, 4, 5, 6$), the overall traffic allocation is 248.5 Tbps (2.9% higher), 238 Tbps (1.3% lesser), 189 Tbps (21.5% lesser), 199 Tbps (17.4% lesser), and 189.5 Tbps (21.54% lesser), respectively.

Fig. 6 and Fig. 7 illustrate the network performance regarding the overall traffic allocation across a spectrum of traffic intensities, specifically with a fixed $BP = 10^{-2}$, within the context of the C+L and C+L+S scenarios, respectively. These figure presents a comparison of the overall network traffic capacity (measured in Tbps - y-axis) as a function of the waveband size (M) for a network utilizing the multi (C+L- and C+L+S-) bands. The configurations tested vary in the number of wavelengths grouped into a single waveband, ranging from 2 to 6 wavelengths per band for uniform traffic requests ranging from 1000 to 7000 Gbps (x-axis). The dots in the plot represents the actual simulation data and the dotted line shows the trend line for particular WB case for all the traffic profiles. As the waveband size increases for the increasing traffic intensity, there is a notable variation in

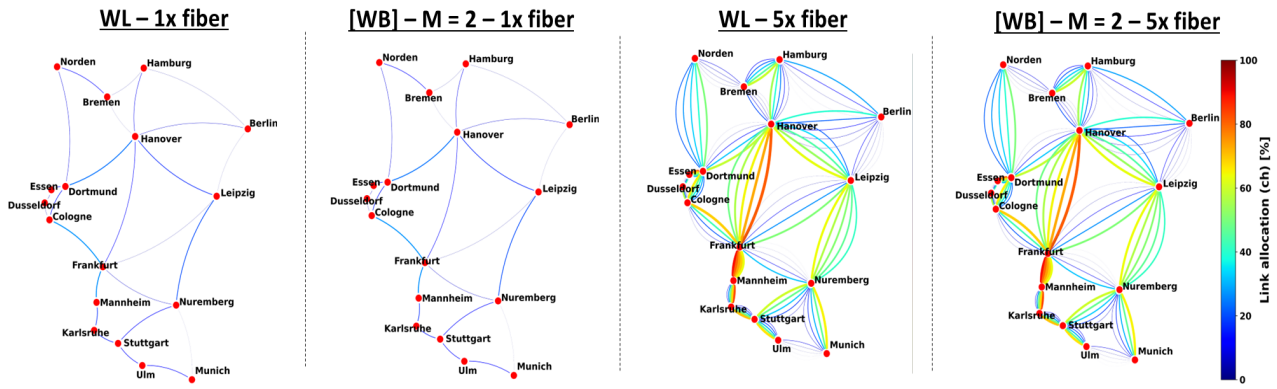

Fig. 8: Heat map of traffic distribution for WL and WB $(M = 2)$ enabled network for 1x vs. 5x fiber.

the network's ability to handle traffic. The steeper downward slope in the conventional WL results in earlier blocking of traffic requests due to limited channel bandwidth. This variation is indicative of the trade-off between the flexibility of wavelength allocation and the efficiency of waveband switching. There is an optimal waveband size for the given traffic profiles, where the network achieves the highest traffic capacity. In Fig. 6, at 2000 Gbps traffic profile, conventional WL allocates around 190 Tbps network traffic, the allocation is of the order $conv.WL > 3WB/WL > 2WB/WL > 5WB/WL > 4WB/WL > 6WB/WL$. For 6000 Gbps case, overall network traffic allocation is of the order $5WB/WL > 2WB/WL > 4WB/WL > 6WB/WL > 3WB/WL$. At lower traffic intensities, the conventional WL switching offers superior granularity and flexibility in routing individual wavelength channels. This finer granularity allows for more efficient utilization of available spectral resources, minimizing wasted bandwidth and reducing the likelihood of blocking under moderate traffic loads. As traffic demand increases, the advantages of appropriately configured waveband switching become more evident, reducing fragmentation and maximizing spectral utilization, which translates to better overall network performance compared to the conventional WL approach. This indicates a balance between the granularity of switching and the overhead associated with waveband formation and management. Fig. 7 shows the same scenarios for the C+L+S- bands, providing overall larger bandwidth. The impact of waveband size on traffic capacity differ from the C+L network scenario due to the added complexity and the potential for increased bandwidth which results in less blocking.

Both figures underscore the importance of WB size in optimizing network performance for multi-band optical networks. They highlight the need for a careful balance between the granularity of control offered by smaller wavebands and the efficiency and scalability benefits of larger wavebands. The analysis demonstrates that the optimal waveband size can significantly affect the network's capacity to manage traffic, with implications for network design and operation in bandwidth-intensive environments.

TABLE I: Overall traffic statistics for for WL and WB $(M = 2)$ for 1x vs. 5x fiber.

Traffic intensity	Fiber	WL	WB $(M = 2)$	
4000 Gbps	1x	241.5	248.5	2.93%
	5x	1591.9	1679.02	5.47%
		≈6.59x	≈ 6.75x	
7000 Gbps	1x	104.84 Tbps	207.9 Tbps	98.35%
	5x	1372.1 Tbps	1524.45 Tbps	11.1%
		≈ 13.7x	≈ 7.3x	

The Fig. 8 compares traffic allocation per link between the WL and WB architectures with $M = 2$. This analysis is performed for the single-fiber (1x) and multi-fiber (5x) scenarios at 7000 Tbps case. The heatmap shows the intensity of traffic, where the color spectrum ranges from blue (indicating 0% traffic allocation) to red (indicating 100% traffic allocation) for each link in the network. At the Frankfurt – Mannheim link, the maximum traffic allocation is observed to be 17.9 Tbps for the WB ($M = 2$ and 5x fiber) case against fiber no. 1, which is represented by 100% and all the other links are accordingly normalized. Tab. I shows the total traffic allocation for two separate cases of traffic intensity (4000 Gbps and 7000 Gbps). The traffic allocation is compared between WL and WB $(M = 2)$ cases and the two fiber cases (1x and 5x). For the 4000 Gbps case, the difference between the WL and WB is 2.9%, whereas for the 7000 Gbps case, the same difference is observed, i.e., 98.35%. This shows that the WB architecture's potentiality signifies the higher traffic request. Also, the difference in the traffic allocation in terms of the ratios for the 1x and 5x fibers implies higher traffic requests.

V. Conclusion

The continuously rising demand for high capacity networks to implement bandwidth-hungry technologies stresses the necessity for robust solutions that can effectively fulfill these upcoming bandwidth requirements. This study presented an in-depth analysis of the performance of WB switching in

comparison to conventional WL switching and its profound impact on the broader networking landscape. The findings indicate that WB switching offers notable advantages over traditional wavelength switching methodologies in high-traffic intensity networks. While conventional wavelength routing may still be viable in certain scenarios, waveband switching presents a more scalable and efficient approach, making it a strong candidate for future bandwidth-abundant optical networks.

ACKNOWLEDGEMENTS

The presented work has been partially supported by the Italian National Recovery and Resilience Plan (NRRP) of NextGenerationEU, a partnership on "Telecommunications of the Future" (PE00000001 - program "RESTART")

REFERENCES

[1] Cisco, "Cisco annual internet report (2018–2023) white paper," (2020).
[2] ITU-T, "G.694.1 spectral grids for wdm applications: Dwdm frequency grids," (2021).
[3] R.-J. Essiambre, G. Kramer, P. J. Winzer, G. J. Foschini, and B. Goebel, "Capacity limits of optical fiber networks," Journal of Lightwave Technology **28**, 662–701 (2010).
[4] R.-J. Essiambre and R. W. Tkach, "Capacity trends and limits of optical communication networks," Proceedings of the IEEE **100**, 1035–1055 (2012).
[5] D. Uzunidis, E. Kosmatos, C. Matrakidis, A. Stavdas, and A. Lord, "Strategies for upgrading an operator's backbone network beyond the c-band: Towards multi-band optical networks," IEEE Photonics Journal **13**, 1–18 (2021).
[6] T. Kobayashi, M. Nakamura, F. Hamaoka, K. Shibahara, T. Mizuno, A. Sano, H. Kawakami, A. Isoda, M. Nagatani, H. Yamazaki, Y. Miyamoto, Y. Amma, Y. Sasaki, K. Takenaga, K. Aikawa, K. Saitoh, Y. Jung, D. J. Richardson, K. Pulverer, M. Bohn, M. Nooruzzaman, and T. Morioka, "1-pb/s (32 sdm/46 wdm/768 gb/s) c-band dense sdm transmission over 205.6-km of single-mode heterogeneous multi-core fiber using 96-gbaud pdm-16qam channels," in *2017 Optical Fiber Communications Conference and Exhibition (OFC),* (2017), pp. 1–3.
[7] K. Saitoh, "Multi-core fiber technology for sdm: Coupling mechanisms and design," Journal of Lightwave Technology **40**, 1527–1543 (2022).
[8] M. Jinno, T. Kodama, and T. Ishikawa, "Principle, design, and prototyping of core selective switch using free-space optics for spatial channel network," Journal of Lightwave Technology **38**, 4895–4905 (2020).
[9] H. Takeshita, K. Matsumoto, S. Yanagimachi, and E. L. T. de Gabory, "Configurations of pump injection and reinjection for improved amplification efficiency of turbo cladding pumped mc-edfa," Journal of Lightwave Technology **38**, 2922–2929 (2020).
[10] D. M. Marom, P. D. Colbourne, A. D'errico, N. K. Fontaine, Y. Ikuma, R. Proietti, L. Zong, J. M. Rivas-Moscoso, and I. Tomkos, "Survey of photonic switching architectures and technologies in support of spatially and spectrally flexible optical networking," Journal of Optical Communications and Networking **9**, 1–26 (2017).
[11] L. Tunesi, I. Khan, M. U. Masood, E. Ghillino, V. Curri, A. Carena, and P. Bardella, "Design and performance assessment of modular multi-band photonic-integrated wss," Opt. Express **31**, 36486–36502 (2023).
[12] H. Hasegawa, "Bandwidth abundant optical networking enabled by spatially-jointed and multi-band flexible waveband routing," IEICE Transactions on Communications (2023).
[13] T. Matsuo, R. Shiraki, Y. Mori, and H. Hasegawa, "Architecture and performance evaluation of fiber-granularity routing networks with supplemental grooming by wavelength conversion," J. Opt. Commun. Netw. **15**, 541–552 (2023).
[14] R. Munakata *et al.*, "Architecture and performance evaluation of bundled-path-routing multi-band optical networks," in *OFC,* (IEEE, 2023), pp. 1–3.
[15] H.-C. Le, H. Hasegawa, and K.-i. Sato, "Large capacity optical networks applying multi-stage hetero-granular optical path routing," Optical Switching and Networking **11**, 105–112 (2014).
[16] T. Ogawa, H. Hasegawa, and K.-i. Sato, "Optical fast circuit switching networks employing dynamic waveband tunnel," IEICE transactions on communications **95**, 3139–3148 (2012).
[17] T. Kuno, Y. Mori, S. Subramaniam, M. Jinno, and H. Hasegawa, "Experimental evaluation of optical cross-connects with flexible waveband routing function for sdm networks," in *2021 Optical Fiber Communications Conference and Exhibition (OFC),* (IEEE, 2021), pp. 1–3.
[18] J. Wu, S. Subramaniam, and H. Hasegawa, "Comparison of oxc node architectures for wdm and flex-grid optical networks," in *2015 24th International Conference on Computer Communication and Networks (ICCCN),* (2015), pp. 1–8.
[19] K. Ishii, H. Hasegawa, K.-i. Sato, S. Kamei, H. Takahashi, and M. Okuno, "Monolithically integrated waveband selective switch using cyclic awgs," in *2008 34th European Conference on Optical Communication,* (IEEE, 2008), pp. 1–2.
[20] R. Munakata, T. Kuno, Y. Mori, S.-C. Lin, M. Matsuura, S. Subramaniam, and H. Hasegawa, "Architecture and performance evaluation of bundled-path-routing multi-band optical networks," in *Optical Fiber Communication Conference (OFC) 2023,* (Optica Publishing Group, 2023), p. M4G.8.
[21] K. Ueda, M. Niwa, Y. Mori, H. Hasegawa, K.-i. Sato, T. Miyazawa, and H. Harai, "Experimental demonstration of multi-granular optical-path network utilizing wavelength/waveband-selective switches," in *2015 Opto-Electronics and Communications Conference (OECC),* (2015), pp. 1–3.
[22] R. Sadeghi, B. Correia, E. Virgillito, A. Napoli, N. Costa, J. Pedro, and V. Curri, "Performance comparison of translucent C-band and transparent C+L-band network," in *Optical Fiber Communication Conference,* (Optical Society of America, 2021), pp. M3E–4.
[23] M. Cantono, R. Gaudino, and V. Curri, "The statistical network assessment process (snap) to evaluate benefits of amplifiers and transponders' upgrades," in *18th Italian National Conference on Photonic Technologies (Fotonica 2016),* (2016), pp. 1–4.
[24] A. Ferrari, A. Napoli, J. K. Fischer, N. Costa, A. D'Amico, J. Pedro, W. Forysiak, E. Pincemin, A. Lord, A. Stavdas *et al.*, "Assessment on the achievable throughput of multi-band ITU-T G. 652. D fiber transmission systems," J. Light. Technol. **38**, 4279–4291 (2020).
[25] B. Correia, R. Sadeghi, E. Virgillito, A. Napoli, N. Costa, J. Pedro, and V. Curri, "Power control strategies and network performance assessment for C+L+S multiband optical transport," JOCN **13**, 147–157 (2021).
[26] Nokia, "Sixth generation super-coherent photonic service engine (pse-6s)," https://www.nokia.com/networks/optical-networks/pse-6s/#overview. Accessed: 2023-07-09.
[27] V. Curri, A. Carena, A. Arduino, G. Bosco, P. Poggiolini, A. Nespola, and F. Forghieri, "Design strategies and merit of system parameters for uniform uncompensated links supporting Nyquist-WDM transmission," JLT **33**, 3921–3932 (2015).
[28] M. U. Masood, L. Tunesi, I. Khan, B. Correia, R. Sadeghi, E. Ghillino, P. Bardella, A. Carena, and V. Curri, "Networking assessment of roadm architecture based on a photonics integrated wss for 800g multi-band optical transport," J. Opt. Commun. Netw. **15**, E51–E62 (2023).